ViT-TTS: Visual Text-to-Speech with Scalable Diffusion Transformer

Huadai Liu[1]*, **Rongjie Huang**[1]*, **Xuan Lin**[2]*, **Wenqiang Xu**[2], **Maozong Zheng**[2], **Hong Chen**[2],
Jinzheng He[1], **Zhou Zhao**[1†]
Zhejiang University[1], Ant Group[2]
{liuhuadai,rongjiehuang,jinzhenghe,zhaozhou}@zju.edu.cn
{daxuan.lx,yugong.xwq,zhengmaozong.zmz,wuyi.ch}@antgroup.com

Abstract

Text-to-speech(TTS) has undergone remarkable improvements in performance, particularly with the advent of Denoising Diffusion Probabilistic Models (DDPMs). However, the perceived quality of audio depends not solely on its content, pitch, rhythm, and energy, but also on the physical environment. In this work, we propose ViT-TTS, the first visual TTS model with scalable diffusion transformers. ViT-TTS complement the phoneme sequence with the visual information to generate high-perceived audio, opening up new avenues for practical applications of AR and VR to allow a more immersive and realistic audio experience. To mitigate the data scarcity in learning visual acoustic information, we 1) introduce a self-supervised learning framework to enhance both the visual-text encoder and denoiser decoder; 2) leverage the diffusion transformer scalable in terms of parameters and capacity to learn visual scene information. Experimental results demonstrate that ViT-TTS achieves new state-of-the-art results, outperforming cascaded systems and other baselines regardless of the visibility of the scene. With low-resource data (1h, 2h, 5h), ViT-TTS achieves comparative results with rich-resource baselines. [1] [2]

1 Introduction

Text-to-speech (TTS) (Ren et al., 2019; Huang et al., 2022a,b) aims to synthesize audios that is consistent with the reference samples in terms of semantic meaning, timbre, emotions, and melody, and has shown remarkable advancements with the advent of Denoising Diffusion Probabilistic Models (DDPMs). However, the perceived audio quality is not solely determined by these aspects, as it is also influenced by the surrounding physical environment. For instance, a room with hard surfaces like concrete or glass reflects sound waves, whereas a room with soft surfaces such as carpets or curtains absorbs them. This variance can drastically impact the clarity and quality of the sound we hear.

To ensure an authentic and captivating experience, it is imperative to accurately model the acoustics of a room, particularly in virtual reality (VR) and augmented reality (AR) applications. Recent years have seen a surge in significant research (Li et al., 2022; Radford et al., 2021; Li et al., 2023; Huang et al., 2023b) addressing the language-visual modeling problem. For instance, Li et al. (2022) have proposed a unified video-language pre-training framework for learning robust representation, while Radford et al. (2021) have focused on large-scale image-text pairs pre-training via contrastive learning. Visual TTS open-ups numerous practical applications, including dubbing archival films, providing a more immersive and realistic experience in virtual and augmented reality, or adding appropriate sound effects to games.

Despite the benefits of language-visual approaches, training visual TTS models typically requires a large amount of training data, while there are very few resources providing parallel text-visual-audio data due to the heavy workload. Besides, creating a sound experience that matches the visual content remains challenging when developing AR/VR applications, as it is still unclear how various regions of the image contribute to reverberation and how to incorporate the visual modality as auxiliary information in TTS.

In this work, we formulate the task of visual TTS to generate audio with reverberation effects in target scenarios given a text and environmental image, introducing ViT-TTS to address the issues of data scarcity and room acoustic modeling. To enhance visual-acoustic matching, we 1) propose the visual-

*Equal contributions

†Corresponding author

[1] Audio samples are available at https://ViT-TTS.github.io/.

[2] Code is available at https://github.com/liuhuadai/ViT-TTS/

Proceedings of the 2023 Conference on Empirical Methods in Natural Language Processing, pages 15957–15969
December 6-10, 2023 ©2023 Association for Computational Linguistics

text fusion to integrate visual and textual information, which provides fine-grained language-visual reasoning by attending to regions of the image; 2) leverage transformer architecture to promote the scalability of the diffusion model. Regarding the data shortage challenge, we pre-train the encoder and decoder in a self-supervised manner, showing that large-scale pre-training reduces data requirements for training visual TTS models.

Experiments results demonstrate that ViT-TTS generates speech samples with accurate reverberation effects in target scenarios, achieving new state-of-the-art results in terms of perceptual quality. In addition, we investigate the scalability of ViT-TTS and its performance under low-resource conditions (1h/2h/5h). The main contributions of this work are summarized as follows:

- We propose the first visual Text-to-Speech model ViT-TTS with vision-text fusion, which enables the generation of high-perceived audio that matches the physical environment.
- We show that large-scale pre-training alleviates the data scarcity in training visual TTS models.
- We introduce the diffusion transformer scalable in terms of parameters and capacity to learn visual scene information.
- Experimental results on subjective and objective evaluation demonstrate the state-of-the-art results in terms of perceptual quality. With low-resource data (1h, 2h, 5h), ViT-TTS achieves comparative results with rich-resource baselines.

2 Related Work

2.1 Text-To-Speech

Text-to-Speech(TTS) tasks are divided into two categories: (1) generating a mel-spectrogram from text or phoneme sequence first (Wang et al., 2017; Ren et al., 2019), and then converting the generated spectrum into a waveform via vocoder (Kong et al., 2020; Lee et al., 2022; Huang et al., 2022a); (2) generating audio directly from text (Donahue et al., 2020; Kim et al., 2021). The earlier TTS (Li et al., 2019; Wang et al., 2017) models adopt an autoregressive manner, which suffers from the problem of slow inference speed. As a solution, non-autoregressive models have been proposed to enable fast inference by generating mel-spectrograms in parallel. More recently, Grad-TTS (Popov et al., 2021), DiffSpeech (MoonInTheRiver, 2021), and ProDiff (Huang et al., 2022c) have employed diffusion generative models to generate high-quality audio, but they all rely on the convolutional architecture such as WaveNet (Oord et al., 2016) and U-Net (Ronneberger et al., 2015) as the backbone. In contrast, some studies (Peebles and Xie, 2023; Bao et al., 2023) in image generation tasks have explored transformers (Vaswani et al., 2017) as an alternative to convolutional architectures, achieving competitive results with U-Net. In this paper, we present the first transformer-based diffusion model as an alternative of convolutional architecture. By harnessing the scalable properties of transformers, we enhance the model capacity to more effectively capture visual scene information and promote the model performance.

2.2 Self-supervised Pre-training

There are two main criteria for optimizing speech pre-training: contrastive loss (Oord et al., 2018; Chung and Glass, 2020; Baevski et al., 2020) and masked prediction loss (Devlin et al., 2018). Contrastive loss is used to distinguish between positive and negative samples with respect to a reference sample, while masked prediction loss is originally proposed for natural language processing (Devlin et al., 2018; Lewis et al., 2019) and later applied to speech processing (Baevski et al., 2020; Hsu et al., 2021). Some recent work (Chung et al., 2021) has combined the two approaches, achieving good performance for downstream automatic speech recognition (ASR) tasks. In this work, we leverage the success of self-supervised to enhance both the encoder and decoder to alleviate the data scarcity issue.

2.3 Acoustic Matching

The primary objective of acoustic matching is to convert audio from a source environment into audio that resembles the target environment. In the field of blind estimation (Mack et al., 2020; Xiong et al., 2018; Murgai et al., 2017; Mezghani and Swindlehurst, 2018), acoustic matching is applied to generate a simple room impulse response (RIR) that can be used to synthesize the corresponding target audio using two critical acoustic metrics - the direct-to-reverberant ratio (DRR) (Zahorik, 2002) and the reverberation time 60 (RT60) (Ratnam et al., 2003). The music production community also implements acoustic matching to modify the

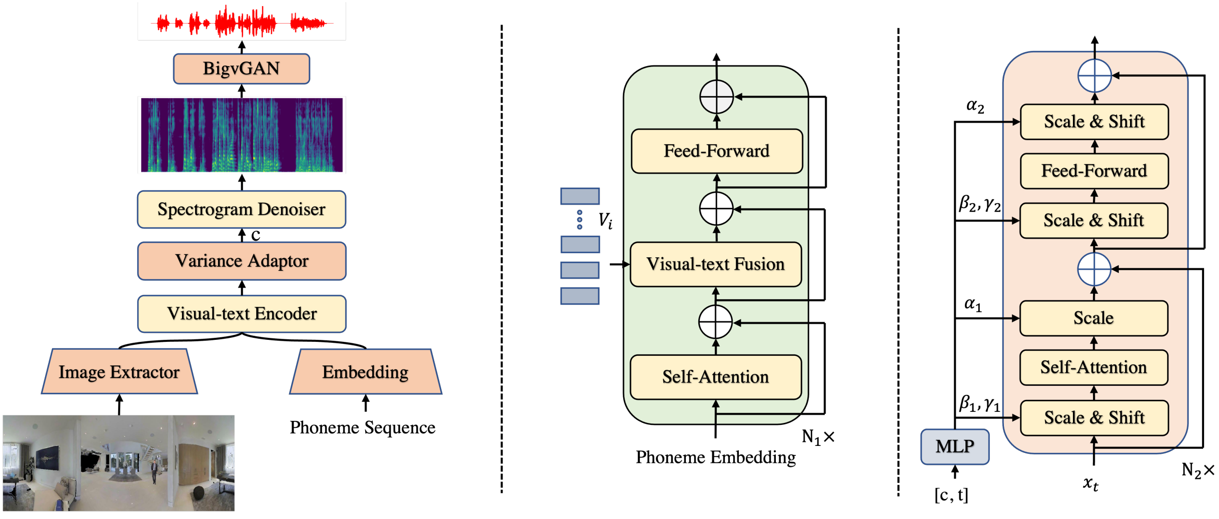

(a) ViT-TTS **(b) Visual-text Encoder** **(c) Spectrogram Denoiser**

Figure 1: The overall architecture for ViT-TTS. In subfigure (b), V_i denotes the visual sequence and N_1 denotes the layers of Encoder. In subfigure (c), N_2 is the number of transformer layers. α and β are the dimension-wise scale parameters, while γ is the dimension-wise shift parameters. c is the variance adaptor's output and t is the diffusion step.

reverberation, thus simulating the reverberation of the target space or processing algorithm (Koo et al., 2021; Sarroff and Michaels, 2020). Recently, there is research on visual acoustic matching (Chen et al., 2022), which involves generating audio recorded in the target environment based on the input source audio clip and an image of the target environment. However, our proposed visual TTS is distinct from those mentioned above as as it aims to generate audio that captures the room acoustics in the target environment based on the written text and the target environment image.

3 Method

3.1 Overview

The overall architecture has been presented as Figure 1. To alleviate the issue of data scarcity, we leverage unlabeled data to pre-train the visual-text encoder and denoiser decoder with scalable transformers in a self-supervised manner. To capture the visual scene information, we employ the visual-text fusion module to reason about how different image patches contribute to texts. BigvGAN (Lee et al., 2022) converts the mel-spectrograms into audio that matches the target scene as a neural vocoder.

3.2 Enhanced visual-text Encoder

Self-supervised Pre-training The advent of the masked language model (Devlin et al., 2018; Clark et al., 2020) has marked a significant milestone in the field of natural language processing. To alleviate the data scarcity issue (Huang et al., 2022d; Liu et al., 2023; Huang et al., 2023c) and learn robust contextual encoder, we are encouraged to adopt the masking strategy like BERT in the pre-training stage. Specifically, we randomly mask the 15% of each phoneme sequence and predict those masked tokens rather than reconstructing the entire input. The masked phoneme sequence is then input into the text encoder to obtain hidden states. The final hidden states are fed into a linear projection layer over the vocabulary to obtain the predicted tokens. Finally, we calculate the cross entropy loss between the predicted tokens and target tokens.

The masked token during the pre-training phase will not be used in the fine-tuning phase. To mitigate this mismatch between the pre-training and fine-tuning, we randomly choose the phonemes to be masked: 1) 80% probability to add masks; 2) 10% probability to keep phoneme unchanged, and 3) 10% probability to replace with a random token in the dictionary.

Visual-Text Fusion In the fine-tuning stage, we integrate the visual modal and module into the encoder to integrate visual and textual information. Before feeding into the visual-text encoder, we first extract image features of panoramic images through ResNet18 (Oord et al., 2018) and obtain phoneme embedding. Both the image features and phoneme embedding are fed into one of the variants of the transformer to get the hidden sequences. Specifically, we first pass the phoneme through relative self-attention, which is defined as follows:

$$\alpha(i,j) = Softmax(\frac{(Q_i W^Q)(K_j W^K + R_{ij})^T}{\sqrt{d_k}}) \tag{1}$$

where n is the length of phoneme embedding, R_{ij} are the relative position embedding of key and value, d_k is the dimension of key, and Q, K, V are all the phoneme embedding. We use relative self-attention to model how much phoneme p_i attends to phoneme p_j. After that, we choose to use cross-attention instead of a simplistic concatenation approach as we can reason about how different image patches contribute to the text after feature extraction. The equation is defined as follows:

$$\delta(V,P) = Softmax(\frac{PV^T}{\sqrt{d_v}})V \tag{2}$$

where P is the phoneme embedding, V is the visual features, and d_v is the dimension of vision features. Finally, the feed-forward layer is applied to output the hidden sequence.

3.3 Enhanced Diffusion Transformer

Scalable Transformer As a rapidly growing category of generative models, DDPMs have demonstrated their exceptional ability to deliver top-notch results in both image (Zhang and Agrawala, 2023; Ho and Salimans, 2022) and audio synthesis (Huang et al., 2022c, 2023a; Lam et al., 2021). However, the most dominant diffusion TTS models adopt a convolutional architecture like WaveNet or U-Net as the de-factor choice of backbone. This architectural choice limits the model scalability to effectively incorporate panoramic visual images. Recent research (Peebles and Xie, 2023; Bao et al., 2023) in the image synthesis field has revealed that the inductive bias of convolutional structures is not a critical determinant of DDPMs' performance. Instead, transformers have emerged as a viable alternative.

For this reason, we propose a diffusion transformer that leverages the scalability of transformers to expand model capacity and incorporate room acoustic information. Moreover, we leverage the adaptive normalization layers in GANs and initialize the full transformer block as the identity function to enhance the transformer architecture.

Unconditional Pre-training In this part, we investigate self-supervised learning from orders of magnitude mel-spectrograms data to alleviate data scarcity. Specifically, assuming the target mel-spectrogram is $\boldsymbol{x}_0$, we first random select 0.065% of $\boldsymbol{x}_0$ as starting indices and apply a mask that spans 10 steps following the Wav2vec2.0 (Baevski et al., 2020). Then, we obtain $\boldsymbol{x}_t$ through a diffusion process, which is defined by a fixed Markov chain from data $\boldsymbol{x}_0$ to the latent variable $\boldsymbol{x}_t$.

$$q(\boldsymbol{x}_1, \cdots, \boldsymbol{x}_T | \boldsymbol{x}_0) = \prod_{t=1}^{T} q(\boldsymbol{x}_t | \boldsymbol{x}_{t-1}), \tag{3}$$

At each diffusion step $t \in [1, T]$, a tiny Gaussian noise is added to $\boldsymbol{x}_{t-1}$ to obtain $\boldsymbol{x}_t$, according to a small positive constant β_t:

$$q(\boldsymbol{x}_t | \boldsymbol{x}_{t-1}) := \mathcal{N}(\boldsymbol{x}_t; \sqrt{1-\beta_t}\boldsymbol{x}_{t-1}, \beta_t \mathbf{I}) \tag{4}$$

x_t obtained from the diffusion process is passed through the transformer to predict Gaussian noise $\boldsymbol{\epsilon}_\theta$. Loss is defined as mean squared error in the $\boldsymbol{\epsilon}$ space, and efficient training is optimizing a random term of t with stochastic gradient descent:

$$\mathcal{L}_\theta^{\text{Grad}} = \left\| \boldsymbol{\epsilon}_\theta \left(\alpha_t \boldsymbol{x}_0 + \sqrt{1-\alpha_t^2}\boldsymbol{\epsilon} \right) - \boldsymbol{\epsilon} \right\|_2^2, \boldsymbol{\epsilon} \sim \mathcal{N}(\mathbf{0}, \mathbf{I}) \tag{5}$$

To this end, ViT-TTS takes advantage of the reconstruction loss to predict the self-supervised representations which largely alleviates the challenges of data scarcity. Detailed formulation of DDPM has been attached in Appendix C.

Controllable Fine-tuning During the fine-tuning stage, we will face the following challenges: (1) there is a data scarcity issue with the available panoramic images and target environmental audio for training; (2) a fast training method is equally crucial for optimizing the diffusion model, as it can save a significant amount of time and storage space. To address these challenges, we draw inspiration from Zhang and Agrawala (2023) and implement a swift fine-tuning technique. Specifically, we create two copies of the pre-trained diffusion model weights, namely a "trainable copy" and a "locked copy," to learn the input conditions. We fix all parameters of the pre-trained transformer, designated as Θ, and duplicate them into a trainable parameter Θ_t. We train these trainable parameters and connect them with the "locked copy" via zero convolution layers. These convolution layers are unique as they have a kernel size of one by one and weights and biases set to zero, progressively growing from zeros to optimized parameters in a learned fashion.

3.4 Architecture

As illustrated in Figure 1, our model comprises a visual-text encoder, variance adaptor, and spectrogram denoiser. The visual-text encoder converts phoneme embeddings and visual features into hidden sequences, while the variance adaptor predicts the duration of each hidden sequence to regulate the length of the hidden sequences to match that of speech frames. Furthermore, different variances like pitch and speaker embedding are incorporated with hidden sequences following FastSpeech 2 Ren et al. (2022). Finally, the spectrogram denoiser iteratively refines the length-regulated hidden states into mel-spectrograms. We put more details in Appendix B.

Visual-Text Encoder The visual-text encoder consists of relative position transformer blocks based on the transformer architecture. Specifically, it convolves a pre-net for phoneme embedding, a visual feature extractor for image, and a transformer encoder which includes multi-head self-attention, multi-head cross-attention, and feed-forward layer.

Variance Adaptor In variance adaptor, the duration and pitch predictors share a similar model structure consisting of a 2-layer 1D-convolutional network with ReLU activation, each followed by the layer normalization and the dropout layer, and an extra linear layer to project the hidden states into the output sequence.

Spectrogram Denoiser Spectrogram denoiser takes in $\boldsymbol{x}_t$ as input to predict $\boldsymbol{\epsilon}$ added in diffusion process conditioned on the step embedding E_t and encoder output. We adopt a variant of the transformer as our backbone and make some improvements upon the standard transformer motivated by Peebles and Xie (2023), mainly includes:(1) we explore replacing standard layer norm layers in transformer blocks with adaptive layer norm (adaLN) to regress scale and shift parameters from the sum of the embedding vector of t and hidden sequence. (2) Inspired by ResNets (Oord et al., 2018), we initialize the transformer block as the identity function and initialize the MLP to output the zero-vector.

3.5 Pre-training, Fine-tuning, and Inference Procedures

Pre-training The pre-training has two stages: 1) encoder stage: pre-train the visual-text encoder vias masked LM loss $\mathcal{L}_{CE}$ (ie. cross-entropy loss) to predict the masked tokens. 2) decoder stage: the masked $\boldsymbol{x}_0$ is puted into denoiser to predict Gaussian noise $\boldsymbol{\epsilon}_\theta$. Then, the Mean Square Error(MSE) loss is applied to the predicted Gaussian noise and target Gaussian noise.

Fine-tuning We begin by loading model weights from the pre-trained visual-text encoder and unconditional diffusion decoder, after which we finetune both of them until the model converges. The final loss term consists of the following parts: (1) sample reconstruction loss $\mathcal{L}_\theta$: MSE between the predicted Gaussian noise and target Gaussian noise. (2) variance reconstruction loss $\mathcal{L}_{dur}, \mathcal{L}_p$: MSE between the predicted and the target phoneme-level duration, pitch.

Inference During inference, DDPM iteratively runs the reverse process to obtain the data sample $\boldsymbol{x}_0$, and then we use a pre-trained BigvGAN-16khz-80band as the vocoder to transform the generated mel-spectrograms into waveforms.

4 Experiment

4.1 Experimental Setup

Dataset We use the SoundSpaces-Speech dataset (Chen et al., 2023), which is constructed on the SoundSpaces platform based on real-world 3D scans to obtain environmental audio. The dataset includes 28,853/1,441/1,489 samples for training/validation/testing, each consisting of clean text, reverberant audio, and panoramic camera angle images. Following (Chen et al., 2022), we remove out-of-view samples and divide the test set into test-unseen and test-seen, where the unseen set injects room acoustics depicted in novel images while the seen set only contains the scenes we have seen in the training stage. We convert the text sequence into the phoneme sequence with an open-source grapheme-to-phoneme conversion tool (Sun et al., 2019) [3].

Following the common pratice (Ren et al., 2019; MoonInTheRiver, 2021), we conduct preprocessing on the speech and text data: 1) extract the spectrogram with the FFT size of 1024, hop size of 256, and window size of 1024 samples; 2) convert it to a mel-spectrogram with 80 frequency bins; and 3) extract F0 (fundamental frequency) from the raw waveform using Parselmouth tool [4].

[3] https://github.com/Kyubyong/g2p

[4] https://github.com/YannickJadoul/Parselmouth

Method	Test-Seen			Test-Unseen			Params
	MOS(↑)	RTE (↓)	MCD (↓)	MOS(↑)	RTE (↓)	MCD (↓)	
GT	4.34±0.07	/	/	4.24±0.07	/	/	/
GT (voc.)	4.18±0.05	0.006	1.46	4.19±0.07	0.008	1.50	/
WaveNet	3.85±0.09	0.091	4.61	3.78±0.12	0.110	4.69	42.3M
Transformer-S	3.92±0.07	0.068	4.57	3.80±0.06	0.077	4.68	32.38M
Transformer-B	3.98±0.06	0.061	4.53	3.90±0.07	0.066	4.62	41.36M
Transformer-L	4.02±0.08	0.056	4.37	3.95±0.07	0.061	4.50	56.96M
Transformer-XL	**4.05±0.07**	**0.047**	**4.35**	**4.00±0.05**	**0.053**	**4.39**	115.12M

Table 1: Comparison between the diffusion WaveNet and diffusion transformers sweeping over model config(S, B, L, XL). All models remove the pre-training stage and other conditions not related to backbone in training and inference remain the same.

Model Configurations The size of the phoneme vocabulary is 73. The dimension of phoneme embeddings and the hidden size of the visual-text transformer block are both 256. We use the pre-trained ResNet18 as an image feature extractor. As for the pitch encoder, the size of the lookup table and encoded pitch embedding are set to 300 and 256. In the denoiser, the number of transformer-B layers is 5 with the hidden size 384 and head 12. We initialize each transformer block as the identity function and set T to 100 and β to constants increasing linearly from $\beta_1 = 10^{-4}$ to $\beta_T = 0.06$. We have attached more detailed information on the model configuration in Appendix B

Pre-training, Fine-tuning, and Inference During the pre-training stage, we pre-train the encoder for 120k steps and the decoder for 160k until convergence. The diffusion probabilistic models have been trained using 1 NVIDIA A100 GPU with a batch size of 48 sentences. In the inference stage, we uniformly use a pre-trained BigvGAN-16khz-80band (Lee et al., 2022) as a vocoder to transform the generated mel-spectrograms into waveforms.

4.2 Scalable Diffusion Transformer

We compare and examine diffusion transformer sweeping over model config(S, B, L, XL), and conduct evaluations in terms of audio quality and parameters. Appendix A gives the details of the model configs. The results have been shown in Table 1. We have some observations from the results: (1) Increasing the depth and number of layers in the transformer can significantly enhance the performance of the diffusion model, resulting in an improvement in both objective metrics and subjective metrics, which demonstrates that expanding the model size enables finer-grained room acoustic modeling. (2) Our proposed diffusion transformer outperforms WaveNet backbone under similar parameters across both test-unseen and test-seen sets, significantly in the rt60 metric. We attribute this to the fact that instead of directly concatenating the condition input like WaveNet, we replace standard layer norm layers in transformer blocks with adaptive layer norm to regress dimension-wise scale and shift parameters from the sum of the embedding vectors of diffusion step and encoder output, which can better incorporate the conditional information, as proven in GANs (Brock et al., 2018; Karras et al., 2019).

4.3 Model Performances

In this study, we conduct a comprehensive comparison of the generated audio quality with other systems, including 1) GT, the ground-truth audio; 2) GT(voc.), where we first convert the groud-truth audio into mel-spectrograms and then convert them to audio using BigvGAN; 3) DiffSpeech (MoonInTheRiver, 2021), one of the most popular DDPM based on WaveNet; 4)ProDiff (Huang et al., 2022c), a recent generator-based diffusion model proposed to reduce the sampling time; 5)Visual-DiffSpeech, incorporate visual-text fusion module into DiffSpeech; 6) Cascaded, the system composed of DiffSpeech and Visual Acoustic Matching(VAM) (Chen et al., 2022). The results, compiled and presented in Table 2, provide valuable insights into the effectiveness of our approach:

(1) As expected, the results in the test-unseen set do poorer than the test-seen part because there are invisible scenarios among the test-unseen set. However, our proposed model has achieved the best performance compared to baseline systems in both sets, indicating that our model generates the best-perceived audio that matches the target envi-

Method	Test-Seen			Test-Unseen			Params
	MOS (↑)	RTE (↓)	MCD (↓)	MOS (↑)	RTE (↓)	MCD (↓)	
GT	4.34±0.07	/	/	4.24±0.07	/	/	/
GT(voc.)	4.18±0.05	0.006	1.46	4.19±0.07	0.008	1.50	/
DiffSpeech	3.79±0.08	0.104	4.65	3.67±0.05	0.120	4.71	29.9M
ProDiff	3.76±0.13	0.121	4.67	3.65±0.06	0.137	4.72	29.9M
Visual-DiffSpeech	3.85±0.09	0.091	4.61	3.78±0.12	0.110	4.69	42.3M
Cascaded	3.61±0.08	0.071	5.13	3.59±0.08	0.082	5.25	146.5M
ViT-TTS	**3.95±0.06**	**0.066**	**4.52**	**3.86±0.05**	**0.076**	**4.59**	41.3M

Table 2: Comparison with baselines on the SoundSpaces-Speech for Seen and Unseen scenarios. The diffusion step of all diffusion models is set to 100. We use the pre-trained model provided by VAM for the evaluation of cascaded.

ronment from written text. (2) Our model surpassed TTS diffusion models(i.e.DiffSpeech and ProDiff) across all metric scores, especially in terms of RTE values. This suggests that conventional diffusion models in TTS do poorly in modeling room acoustic information, as they mainly focus on audio content, pitch, energy, etc. Our proposed visual-text fusion module addresses this challenge by injecting visual properties into the model, resulting in a more accurate prediction of the correct acoustics from images and high-perceived audio synthesis. (3) The results of comparison with Visual-DiffSpeech highlight the advantages of our choice of transformer and self-supervised pre-training. Although Visual-DiffSpeech adds the visual-text module, the choice of WaveNet and the lack of a self-supervised pre-training strategy make it perform worse in predicting the correct acoustics from images and synthesizing high-perceived audio. (4) The cascaded system composed of DiffSpeech and Visual Acoustic Matching model visual properties is better than other baselines. However, compared to our proposed model, it performed worse in both test-unseen and test-seen environments. This suggests that our direct visual text-to-speech system eliminates the influence of error propagation caused by the cascaded manner, resulting in high-perceived audio. In conclusion, our comprehensive evaluation results demonstrate the effectiveness of our proposed model in generating high-quality audio that matches the target environment.

4.4 Low Resource Evaluation

Training visual text-to-speech models typically requires a large amount of parallel target environment image and audio training data, while there may be very few resources due to the heavy workload. In this section, we prepare low-resource audio-visual data (1h/2h/5h) and leverage large-scale text-only and audio-only data to boost the performance of the visual TTS system, to investigate the effectiveness of our self-supervised learning methods. The results are compiled and presented in Table 3, and we have the following observations: 1)As training data is reduced in the low-resource scenario, a distinct degradation in generated audio quality could be witnessed in both test sets (test-seen and test-unseen). 2) Leveraging orders of magnitude text-only and audio-only data with self-supervised learning, the ViT-TTS achieve RTE scores of 0.082 and 0.068 respectively in test-unseen and test-seen, showing a significant promotion regardless of the unseen scene. In this way, the dependence on a large number of parallel audio-visual data can be reduced for constructing visual text-to-speech systems.

Method	MOS (↑)	RTE (↓)	MCD (↓)
Finetune with 1 hour data			
Test-Seen	3.72±0.05	0.092	5.04
Test-Unseen	3.67±0.06	0.101	5.11
Finetune with 2 hours data			
Test-Seen	3.75±0.06	0.089	4.85
Test-Unseen	3.70±0.07	0.097	4.89
Finetune with 5 hours data			
Test-Seen	3.83±0.05	0.068	4.65
Test-Unseen	3.73±0.09	0.082	4.72

Table 3: Low resource evaluation results.

4.5 Case Study

We provide two examples of generation sampled from a large empty room with significant reverberation in the Test-Seen environment depicted in Figure 2, and have the following observations: 1)

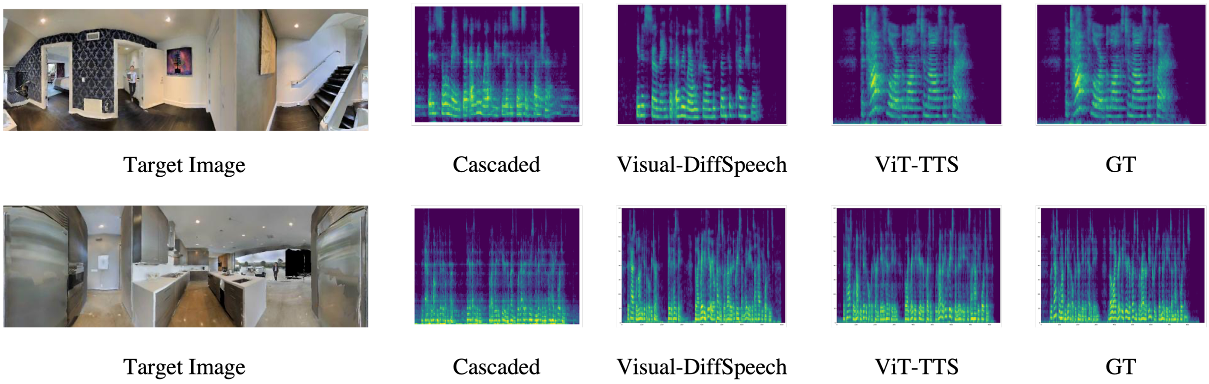

Target Image Cascaded Visual-DiffSpeech ViT-TTS GT

Target Image Cascaded Visual-DiffSpeech ViT-TTS GT

Figure 2: Visualizations of the ground truth and generated mel-spectrograms by different Visual TTS models. The text corresponding to the first line in test-seen is "it is so made that everywhere we feel the sense of punishment" while the second line in test-unseen is "the task will not be difficult returned david hesitating though i greatly fear your presence would rather increase than mitigate his unhappy fortunes ".

Mel-spectrograms produced by ViT-TTS are noticeably more similar to the target counterpart. 2) Moreover in challenging scenarios with invisible scene images, cascaded systems suffer severely from the issue of noisy and reverb details missing, which is largely alleviated in ViT-TTS.

4.6 Ablation Studies

We conduct ablation studies to demonstrate the effectiveness of several key techniques on the Test-Unseen set in our model, including the encoder pre-training(EP), decoder pre-training(DP), visual input, random image, and concat function. The results of both subjective and objective evaluations have been presented in Table 4, and we have the following observations: 1) Removing the self-supervised encoder and decoder pre-training strategy results in a decline in all indicators, which demonstrates the effectiveness and efficiency of the proposed pre-training strategy in reducing data variance and promoting model convergence. 2) Without the input of RGB-D image and removing all of the modules related to the image causes a distinct degradation in RTE values, which demonstrates that our model successfully learns acoustics from the visual scene. 3) The replacement of cross-attention with the concat fusion function results in a decrease in performance across all metrics, highlighting the effectiveness of our visual-text fusion module.

Furthermore, we conducted a more detailed exploration of our model's processing and reasoning about different patches in the RGB-D images. To achieve this, we deliberately substituted the target image with random images, allowing us to determine whether the model can derive meaningful representations from visual inputs. Our findings show that after replacing the target image with a random image, the performance of our model significantly degraded, indicating that our model could model the room acoustic information of visual input.

Method	MOS (↑)	RTE (↓)	MCD (↓)
GT(voc.)	4.18±0.07	0.008	1.50
ViT-TTS	**3.86±0.05**	**0.076**	**4.59**
w/o EP	3.82±0.07	0.078	4.63
w/o DP	3.83±0.06	0.081	4.65
w/o Visual	3.78±0.07	0.102	4.68
w/ RI	3.73±0.08	0.103	4.75
w/ Concat	3.80 ±0.06	0.089	4.63

Table 4: Ablation study results. EP, DP, and RI are encoder pre-training, decoder pre-training, and random images respectively.

5 Conclusion

In this paper, we proposed ViT-TTS, the first visual text-to-speech synthesis model that aimed to convert written text and target environmental images into audio that matches the target environment. To mitigate the data scarcity for training visual TTS tasks and model visual acoustic information, we 1) introduced a self-supervised learning framework to enhance both the visual-text encoder and denoiser decoder; 2) leveraged the diffusion transformer scalable in terms of parameters and capacity to improve performance.

Experimental results demonstrated that ViT-TTS achieved new state-of-the-art results and performed comparably to rich-resource baselines even with limited data. To this end, ViT-TTS provided a solid foundation for future visual text-to-speech studies, and we envision that our approach will have far-reaching impacts on the fields of AR and VR.

6 Limitation and Potential Risks

As indicated in the experimental setup, we utilized ResNet-18 as our image feature extractor. While it is a classic extractor, there may be newer extractors that perform better. In future work, we will explore the use of superior extractors to enhance the quality of generated audio.

Moreover, our pre-trained encoder and decoder are based on the SoundSpace-Speech dataset, which, as described in the dataset section, is not sufficiently large. To address this limitation in future work, we will pre-train on a large-scale dataset to achieve better performance in low-resource scenarios.

ViT-TTS lowers the requirements for visual text-to-speech generation, which may cause fraud and scams by impersonating someone else's voice. Furthermore, there is the potential for leading to the spread of false information and rumors.

Acknowledgements

This work was supported in part by the National Natural Science Foundation of China under Grant No.61836002 and Ant Group Research Fund.

References

Alexei Baevski, Yuhao Zhou, Abdelrahman Mohamed, and Michael Auli. 2020. wav2vec 2.0: A framework for self-supervised learning of speech representations. *Advances in neural information processing systems*, 33:12449–12460.

Fan Bao, Shen Nie, Kaiwen Xue, Chongxuan Li, Shi Pu, Yaole Wang, Gang Yue, Yue Cao, Hang Su, and Jun Zhu. 2023. One transformer fits all distributions in multi-modal diffusion at scale. *arXiv preprint arXiv:2303.06555*.

Andrew Brock, Jeff Donahue, and Karen Simonyan. 2018. Large scale gan training for high fidelity natural image synthesis. *arXiv preprint arXiv:1809.11096*.

Changan Chen, Ruohan Gao, Paul Calamia, and Kristen Grauman. 2022. Visual acoustic matching. In *Proceedings of the IEEE/CVF Conference on Computer Vision and Pattern Recognition (CVPR)*, pages 18858–18868.

Changan Chen, Wei Sun, David Harwath, and Kristen Grauman. 2023. Learning audio-visual dereverberation.

Yu-An Chung and James Glass. 2020. Improved speech representations with multi-target autoregressive predictive coding. *arXiv preprint arXiv:2004.05274*.

Yu-An Chung, Yu Zhang, Wei Han, Chung-Cheng Chiu, James Qin, Ruoming Pang, and Yonghui Wu. 2021. w2v-bert: Combining contrastive learning and masked language modeling for self-supervised speech pre-training. *2021 IEEE Automatic Speech Recognition and Understanding Workshop (ASRU)*, pages 244–250.

Kevin Clark, Minh-Thang Luong, Quoc V Le, and Christopher D Manning. 2020. Electra: Pre-training text encoders as discriminators rather than generators. *arXiv preprint arXiv:2003.10555*.

Jacob Devlin, Ming-Wei Chang, Kenton Lee, and Kristina Toutanova. 2018. Bert: Pre-training of deep bidirectional transformers for language understanding. *arXiv preprint arXiv:1810.04805*.

Jeff Donahue, Sander Dieleman, Mikołaj Bińkowski, Erich Elsen, and Karen Simonyan. 2020. End-to-end adversarial text-to-speech. *arXiv preprint arXiv:2006.03575*.

Jonathan Ho, Ajay Jain, and Pieter Abbeel. 2020. Denoising diffusion probabilistic models.

Jonathan Ho and Tim Salimans. 2022. Classifier-free diffusion guidance. *arXiv preprint arXiv:2207.12598*.

Wei-Ning Hsu, Benjamin Bolte, Yao-Hung Hubert Tsai, Kushal Lakhotia, Ruslan Salakhutdinov, and Abdelrahman Mohamed. 2021. Hubert: Self-supervised speech representation learning by masked prediction of hidden units. *IEEE/ACM Transactions on Audio, Speech, and Language Processing*, 29:3451–3460.

Rongjie Huang, Jiawei Huang, Dongchao Yang, Yi Ren, Luping Liu, Mingze Li, Zhenhui Ye, Jinglin Liu, Xiang Yin, and Zhou Zhao. 2023a. Make-an-audio: Text-to-audio generation with prompt-enhanced diffusion models. *arXiv preprint arXiv:2301.12661*.

Rongjie Huang, Max WY Lam, Jun Wang, Dan Su, Dong Yu, Yi Ren, and Zhou Zhao. 2022a. Fastdiff: A fast conditional diffusion model for high-quality speech synthesis. *arXiv preprint arXiv:2204.09934*.

Rongjie Huang, Mingze Li, Dongchao Yang, Jiatong Shi, Xuankai Chang, Zhenhui Ye, Yuning Wu, Zhiqing Hong, Jiawei Huang, Jinglin Liu, et al. 2023b. Audiogpt: Understanding and generating speech, music, sound, and talking head. *arXiv preprint arXiv:2304.12995*.

Rongjie Huang, Huadai Liu, Xize Cheng, Yi Ren, Linjun Li, Zhenhui Ye, Jinzheng He, Lichao Zhang, Jinglin Liu, Xiang Yin, and Zhou Zhao. 2023c. Av-transpeech: Audio-visual robust speech-to-speech translation.

Rongjie Huang, Yi Ren, Jinglin Liu, Chenye Cui, and Zhou Zhao. 2022b. Generspeech: Towards style transfer for generalizable out-of-domain text-to-speech. In *Advances in Neural Information Processing Systems*.

Rongjie Huang, Zhou Zhao, Huadai Liu, Jinglin Liu, Chenye Cui, and Yi Ren. 2022c. Prodiff: Progressive fast diffusion model for high-quality text-to-speech. In *Proceedings of the 30th ACM International Conference on Multimedia*, pages 2595–2605.

Rongjie Huang, Zhou Zhao, Jinglin Liu, Huadai Liu, Yi Ren, Lichao Zhang, and Jinzheng He. 2022d. Transpeech: Speech-to-speech translation with bilateral perturbation. *arXiv preprint arXiv:2205.12523*.

Tero Karras, Samuli Laine, and Timo Aila. 2019. A style-based generator architecture for generative adversarial networks. In *Proceedings of the IEEE/CVF conference on computer vision and pattern recognition*, pages 4401–4410.

Jaehyeon Kim, Jungil Kong, and Juhee Son. 2021. Conditional variational autoencoder with adversarial learning for end-to-end text-to-speech. In *International Conference on Machine Learning*, pages 5530–5540. PMLR.

Jungil Kong, Jaehyeon Kim, and Jaekyoung Bae. 2020. Hifi-gan: Generative adversarial networks for efficient and high fidelity speech synthesis. *Proc. of NeurIPS*.

Junghyun Koo, Seungryeol Paik, and Kyogu Lee. 2021. Reverb conversion of mixed vocal tracks using an end-to-end convolutional deep neural network. In *ICASSP 2021-2021 IEEE International Conference on Acoustics, Speech and Signal Processing (ICASSP)*, pages 81–85. IEEE.

Max WY Lam, Jun Wang, Rongjie Huang, Dan Su, and Dong Yu. 2021. Bilateral denoising diffusion models. *arXiv preprint arXiv:2108.11514*.

Sang-gil Lee, Wei Ping, Boris Ginsburg, Bryan Catanzaro, and Sungroh Yoon. 2022. Bigvgan: A universal neural vocoder with large-scale training. *arXiv preprint arXiv:2206.04658*.

Mike Lewis, Yinhan Liu, Naman Goyal, Marjan Ghazvininejad, Abdelrahman Mohamed, Omer Levy, Veselin Stoyanov, and Luke Zettlemoyer. 2019. Bart: Denoising sequence-to-sequence pre-training for natural language generation, translation, and comprehension. In *Annual Meeting of the Association for Computational Linguistics*.

Junnan Li, Dongxu Li, Silvio Savarese, and Steven Hoi. 2023. Blip-2: Bootstrapping language-image pretraining with frozen image encoders and large language models. *arXiv preprint arXiv:2301.12597*.

Junnan Li, Dongxu Li, Caiming Xiong, and Steven Hoi. 2022. Blip: Bootstrapping language-image pretraining for unified vision-language understanding and generation. In *International Conference on Machine Learning*, pages 12888–12900. PMLR.

Naihan Li, Shujie Liu, Yanqing Liu, Sheng Zhao, and Ming Liu. 2019. Neural speech synthesis with transformer network. In *Proceedings of the AAAI Conference on Artificial Intelligence*, volume 33, pages 6706–6713.

Huadai Liu, Rongjie Huang, Jinzheng He, Gang Sun, Ran Shen, Xize Cheng, and Zhou Zhao. 2023. Wav2sql: Direct generalizable speech-to-sql parsing.

Wolfgang Mack, Shuwen Deng, and Emanuël Habets. 2020. Single-channel blind direct-to-reverberation ratio estimation using masking. In *Interspeech*.

Amine Mezghani and A. Lee Swindlehurst. 2018. Blind estimation of sparse broadband massive MIMO channels with ideal and one-bit ADCs. *IEEE Transactions on Signal Processing*, 66(11):2972–2983.

MoonInTheRiver. 2021. Diffsinger. `https://github.com/MoonInTheRiver/DiffSinger`.

Prateek Murgai, Mark Rau, and Jean-Marc Jot. 2017. Blind estimation of the reverberation fingerprint of unknown acoustic environments. *Journal of The Audio Engineering Society*.

Aaron van den Oord, Sander Dieleman, Heiga Zen, Karen Simonyan, Oriol Vinyals, Alex Graves, Nal Kalchbrenner, Andrew Senior, and Koray Kavukcuoglu. 2016. Wavenet: A generative model for raw audio. *arXiv preprint arXiv:1609.03499*.

Aaron van den Oord, Yazhe Li, and Oriol Vinyals. 2018. Representation learning with contrastive predictive coding. *arXiv preprint arXiv:1807.03748*.

William Peebles and Saining Xie. 2023. Scalable diffusion models with transformers.

Vadim Popov, Ivan Vovk, Vladimir Gogoryan, Tasnima Sadekova, and Mikhail Kudinov. 2021. Grad-tts: A diffusion probabilistic model for text-to-speech. In *International Conference on Machine Learning*, pages 8599–8608. PMLR.

Alec Radford, Jong Wook Kim, Chris Hallacy, Aditya Ramesh, Gabriel Goh, Sandhini Agarwal, Girish Sastry, Amanda Askell, Pamela Mishkin, Jack Clark, et al. 2021. Learning transferable visual models from natural language supervision. In *International conference on machine learning*, pages 8748–8763. PMLR.

Rama Ratnam, Douglas L Jones, Bruce C Wheeler, William D O'Brien Jr, Charissa R Lansing, and Albert S Feng. 2003. Blind estimation of reverberation time. *The Journal of the Acoustical Society of America*, 114(5):2877–2892.

Yi Ren, Chenxu Hu, Xu Tan, Tao Qin, Sheng Zhao, Zhou Zhao, and Tie-Yan Liu. 2022. Fastspeech 2: Fast and high-quality end-to-end text to speech.

Yi Ren, Yangjun Ruan, Xu Tan, Tao Qin, Sheng Zhao, Zhou Zhao, and Tie-Yan Liu. 2019. Fastspeech: Fast, robust and controllable text to speech. *Advances in Neural Information Processing Systems*, 32.

Olaf Ronneberger, Philipp Fischer, and Thomas Brox. 2015. U-net: Convolutional networks for biomedical image segmentation. In *Medical Image Computing and Computer-Assisted Intervention–MICCAI 2015: 18th International Conference, Munich, Germany, October 5-9, 2015, Proceedings, Part III 18*, pages 234–241. Springer.

Andy Sarroff and Roth Michaels. 2020. Blind arbitrary reverb matching. In *Proceedings of the 23rd International Conference on Digital Audio Effects (DAFx-2020)*, volume 2.

Manfred R Schroeder. 1965. New method of measuring reverberation time. *The Journal of the Acoustical Society of America*, 37(6):1187–1188.

Hao Sun, Xu Tan, Jun-Wei Gan, Hongzhi Liu, Sheng Zhao, Tao Qin, and Tie-Yan Liu. 2019. Token-level ensemble distillation for grapheme-to-phoneme conversion. *arXiv preprint arXiv:1904.03446*.

Ashish Vaswani, Noam Shazeer, Niki Parmar, Jakob Uszkoreit, Llion Jones, Aidan N. Gomez, Lukasz Kaiser, and Illia Polosukhin. 2017. Attention is all you need.

Yuxuan Wang, RJ Skerry-Ryan, Daisy Stanton, Yonghui Wu, Ron J Weiss, Navdeep Jaitly, Zongheng Yang, Ying Xiao, Zhifeng Chen, Samy Bengio, et al. 2017. Tacotron: Towards end-to-end speech synthesis. *arXiv preprint arXiv:1703.10135*.

Feifei Xiong, Stefan Goetze, Birger Kollmeier, and Bernd T Meyer. 2018. Joint estimation of reverberation time and early-to-late reverberation ratio from single-channel speech signals. *IEEE/ACM Transactions on Audio, Speech, and Language Processing*, 27(2):255–267.

Pavel Zahorik. 2002. Direct-to-reverberant energy ratio sensitivity. *The Journal of the Acoustical Society of America*, 112(5):2110–2117.

Lvmin Zhang and Maneesh Agrawala. 2023. Adding conditional control to text-to-image diffusion models.

A TRANSFORMER CONFIGURATION

The details of transformer denoisers are shown in Table 5, while B, M, L, and XL means the base, medium, large, extra large respectively.

Model	layers	Hidden Size	Heads
Transformer-S	4	256	8
Transformer-B	5	384	12
Transformer-L	6	512	16
Transformer-XL	8	768	16

Table 5: Diffusion Transformer Configs.

B ARCHITECTURE

We list the model hyper-parameters of ViT-TTS in Table 6.

Hyperparameter		ViT-TTS
Visual-Text Encoder	Phoneme Embedding	256
	Pre-net Layers	3
	Pre-net Hidden	256
	Visual Conv2d Kernel	(7, 7)
	Visual Conv2d Stride	(2, 2)
	Encoder Layers	4
	Encoder Hidden	256
	Encoder Conv1d Kernel	9
	Conv1D Filter Size	1024
	Attention Heads	2
	Dropout	0.1
Variance Predictor	Conv1D Kernel	3
	Conv1D Filter Size	256
	Dropout	0.5
Denoiser	Diffusion Embedding	384
	Transformer Layers	5
	Transformer Hidden	384
	Attention Heads	12
	Position Embedding	384
	Scale/Shift Size	384
Total Number of Parameters		41.36M

Table 6: Hyperparameters of ViT-TTS models.

C DIFFUSION POSTERIOR DISTRIBUTION

Firstly we compute the corresponding constants respective to diffusion and reverse process:

$$\alpha_t = \prod_{i=1}^{t} \sqrt{1-\beta_i} \quad \sigma_t = \sqrt{1-\alpha_t^2} \tag{6}$$

The Gaussian posterior in diffusion process is defined through the Markov chain, where each iteration adds Gaussian noise.

$$\begin{aligned} q(\boldsymbol{x}_1, \cdots, \boldsymbol{x}_T | x_0) &= \prod_{t=1}^{T} q(\boldsymbol{x}_t | \boldsymbol{x}_{t-1}), \\ q(\boldsymbol{x}_t | \boldsymbol{x}_{t-1}) &= \mathcal{N}(\boldsymbol{x}_t; \sqrt{1-\beta_t}\boldsymbol{x}_{t-1}, \beta_t \mathbf{I}) \end{aligned} \tag{7}$$

We emphasize the property observed by (Ho et al., 2020), the diffusion process can be computed in a closed form:

$$q(\boldsymbol{x}_t | \boldsymbol{x}_0) = \mathcal{N}(\boldsymbol{x}_t; \alpha_t \boldsymbol{x}_0, \sigma_t \mathbf{I}) \tag{8}$$

Applying Bayes' rule, we can obtain the forward process posterior when conditioned on $\boldsymbol{x}_0$

$$\begin{aligned} q(\boldsymbol{x}_{t-1} | \boldsymbol{x}_t, \boldsymbol{x}_0) &= \frac{q(\boldsymbol{x}_t | \boldsymbol{x}_{t-1}, \boldsymbol{x}_0) q(\boldsymbol{x}_{t-1} | \boldsymbol{x}_0)}{q(\boldsymbol{x}_t | \boldsymbol{x}_0)} \\ &= \mathcal{N}(\boldsymbol{x}_{t-1}; \tilde{\boldsymbol{\mu}}_t(\boldsymbol{x}_t, \boldsymbol{x}_0), \tilde{\beta}_t \mathbf{I}), \end{aligned} \tag{9}$$

where $\tilde{\boldsymbol{\mu}}_t(\boldsymbol{x}_t, \boldsymbol{x}_0) = \frac{\alpha_{t-1}\beta_t}{\sigma_t}\boldsymbol{x}_0 + \frac{\sqrt{1-\beta_t}(\sigma_{t-1})}{\sigma_t}\boldsymbol{x}_t, \quad \tilde{\beta}_t = \frac{\sigma_{t-1}}{\sigma_t}\beta_t$

D DIFFUSION ALGORITHM

See Algorithm 1 and 2.

Algorithm 1 Training procedure

```
Input: The denoiser $\epsilon_\theta$, diffusion step T and variance condition c.
repeat
    Sample $\boldsymbol{x}_0 \sim q_{data}$, $\epsilon \sim \mathcal{N}(\mathbf{0}, \boldsymbol{I})$
    Take gradient descent steps on $\nabla_\theta \|\epsilon - \epsilon_\theta(\sqrt{\overline{\alpha}_t}\boldsymbol{x}_0 + \sqrt{1-\overline{\alpha}_t}\epsilon, c, t)\|$.
until convergence
```

Algorithm 2 Sampling

```
Input: The denoiser $\epsilon_\theta$, and variance condition $c$.
Sample $\boldsymbol{x}_T \sim \mathcal{N}(\mathbf{0}, \boldsymbol{I})$
for $t = T, \cdots, 1$ do
    if t = 1 then
        z = 0
    else
        Sample $\boldsymbol{z} \sim \mathcal{N}(\mathbf{0}, \boldsymbol{I})$
    end if
    Sample $\boldsymbol{x}_{t-1} = \frac{1}{\sqrt{\alpha_t}}(\boldsymbol{x}_t - \frac{1-\alpha_t}{\sqrt{1-\overline{\alpha}_t}}\epsilon_\theta(\boldsymbol{x}_t, c, t)) + \sigma_t \boldsymbol{z}$
end for
```

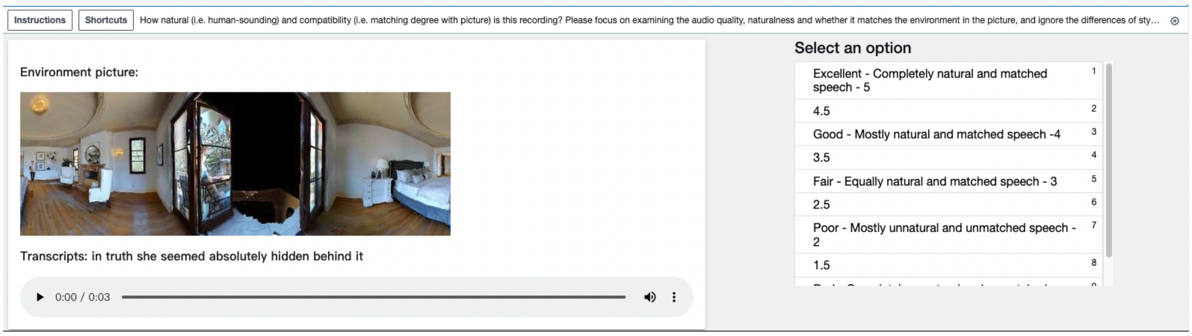

How natural (i.e. human-sounding) and compatibility (i.e. matching degree with picture) is this recording? Please focus on examining the audio quality, naturalness and whether it matches the environment in the picture, and ignore the differences of sty...

Environment picture:

Transcripts: in truth she seemed absolutely hidden behind it

0:00 / 0:03

Select an option

- Excellent - Completely natural and matched speech - 5 1
- 4.5 2
- Good - Mostly natural and matched speech -4 3
- 3.5 4
- Fair - Equally natural and matched speech - 3 5
- 2.5 6
- Poor - Mostly unnatural and unmatched speech - 2 7
- 1.5 8

Figure 3: Screenshots of subjective evaluations.

E EVALUATION MATRIX

E.1 Evaluation Metrics

We measure the sample quality of the generated waveform using both objective metrics and subjective indicators. The objective metrics we collected are designed to measure varied aspects of waveform quality between the ground-truth audio and the generated sample. Following the common practice of (Huang et al., 2022c; MoonInTheRiver, 2021; Popov et al., 2021), we randomly select a part of the test set for objective evaluation, here is 50. We provide the following metrics: (1) **RT60 Error(RTE)**-the correctness of the room acoustics between the predicted waveform and target waveform's RT60 values. RT60 indicates the reverberation time in seconds for the audio signal to decay by 60 dB, a standard metric to characterize room acoustics. We estimate the RT60 directly from magnitude spectrograms of the output audio, using a model trained with disjoint SoundSpaces data. (2) **Mel Cepstral Distortion(MCD)**-measures the spectral distance between the synthesized and reference mel-spectrum features. The utilization of RTE is solely intended for evaluating the room acoustic performance of the generated audio, and as an additional measure, we have incorporated the MCD metric to assess the quality of the mel-spectrogram.

For subjective metrics, we use crowd-sourced human evaluation via Amazon Mechanical Turk, where raters are asked to rate **Mean Opinion Score(MOS)** on a 1-5 Likert scale.

E.2 RT60 Estimator

Following (Chen et al., 2022), we first encode the 2.56s speech clips as spectrograms, process them with a ResNet18 (Oord et al., 2018) and predict the RT60 of the speech. The ground truth RT60 is calculated with the Schroeder (Schroeder, 1965). We optimize the MSE loss between the predicted RT60 and the ground truth RT60.

E.3 MOS Evaluation

To probe audio quality, we conduct the MOS (mean opinion score) tests and explicitly instruct the raters to "focus on examining the audio quality, naturalness and whether the audio matches with the given image.". The testers present and rate the samples, and each tester is asked to evaluate the subjective naturalness on a 1-5 Likert scale.

Our subjective evaluation tests are crowd-sourced and conducted via Amazon Mechanical Turk. These ratings are obtained independently for model samples and reference audio, and both are reported. The screenshots of instructions for testers have been shown in Figure 3. A small subset of speech samples used in the test is available at https://ViT-TTS.github.io/

F LOW RESOURCE SETTING

We partition the training set of SoundSpaces-Speech into 1h/2h/5h subsets based on the alphabetical order of speech IDs. Subsequently, we employ these subsets to fine-tune our pre-trained models and assess their performance on identical test sets.